Engineering Failure Analysis 102 (2019) 160–169

Contents lists available at ScienceDirect

Engineering Failure Analysis

journal homepage: www.elsevier.com/locate/engfailanal

Flow line corrosion failure as a function of operating temperature and CO_2 partial pressure using real time field data

Emeka Emmanuel Okoro[a,*], Adokiye Mercy Kurah[b], Samuel E. Sanni[c], Adewale Dosunmu[d], Evelyn B. Ekeinde[d]

[a] Petroleum Engineering Department, Covenant University Ota, Nigeria
[b] Petrochemical Engineering Department, Rivers State University of Science and Technology, Nigeria
[c] Chemical Engineering Department, Covenant University Ota, Nigeria
[d] Petroleum Engineering Department, University of Port Harcourt, Rivers State, Nigeria

ARTICLE INFO

Keywords:
Internal corrosion
Corrosion failure
Curvilinear pipe
CO_2 partial pressure
Non-linear regression model
Operating temperature

ABSTRACT

A Nonlinear Regression Analytical model was used to simulate the corrosion rate of CO_2 flowing through a pipeline at different operating conditions. The model was formed by applying the simple current-resistance relationship which was further simplified to obtain an appropriate expression for estimating the corrosion rate of a pipeline in relation to the partial pressure of the gas at different temperatures (30–37 °C). Field conditions were validated against simulated results and based on the findings, the model proved to be an accurate tool for determining the corrosion rate of CO_2 for curvilinear pipe of 3 km length transporting fluids having similar gas composition. Based on the estimated corrosion rates, the model's accuracy lies in the range of 96–99%. Also, from the results, there seem to be an approximate linear relationship/positive correlation between the corrosion rate of CO_2 and, the system temperature and CO_2 partial pressure.

1. Introduction

Pipelines whether buried in the ground, exposed to the atmosphere, or submerged in water, are liable to corrosion. Without proper maintenance, every pipeline system will eventually deteriorate, and a corroded pipe is unsafe as a means of transportation because of the associated failure risks [1,2]. These failures in pipelines and flow lines lead to shutdown of facilities and platforms. Corrosion results in the deterioration of a metal and weakens its structural integrity as a result of chemical reactions between it and the surrounding environment [3]. Wang et al. [4] in their study, highlighted and determined the actual corrosion behavior of absorbable metal materials as a vital technological concern. They also emphasized the importance of selecting parameters that have specific applications for the system under consideration.

Corrosion in flow lines occurs where there is loss of metal from an exposed surface in a corrosive environment. Most pipeline failures are due to localized corrosion and its mechanism can be induced by flow, metallurgy, deposits, internal stresses and microbiologically influenced corrosion (MIC) among others [5,6]. The internal corrosion of carbon steel is a noteworthy problem for the oil and gas industry because of its frequency of occurrence. Although high cost corrosion resistant alloys (CRAs) are often developed to resist internal corrosion, carbon steel is still the most cost effective material used for oil and gas production. Issues of possible corrosive species encountered in the oil and gas industry have been documented in so many literature [7–9]. The reports on the

---

[*] Corresponding author.
E-mail address: emeka.okoro@covenantuniversity.edu.ng (E.E. Okoro).

https://doi.org/10.1016/j.engfailanal.2019.04.037
Received 21 August 2018; Received in revised form 14 April 2019; Accepted 15 April 2019

significance of CO_2 in corrosion of metal have also been reported [10,11]; and, there seems to be a consensus on the significance of CO_2 in corrosion of flow lines.

Corrosion control is an ongoing dynamic process; therefore, an effective model for predicting flow line corrosion is essential. Corrosion models provide early warning signs of impending failures; they are developed correlations that relate processes and their corrosive effects on systems which help to diagnose a specific problem and in turn evaluate the effectiveness of any corrosion control measure/prevention technique applied to improve the service life of the target metal. For process piping, a consideration of API 2611 and API 570 will help to understand the process involved in carrying out a world class inspection during pipe selection for specific operations [12]. Damages caused by external corrosion, except for corrosion under insulation (CUI), are most easily accessed by visual inspection. Kain [13] extensively studied the forms and mechanisms of flow induced corrosion, and also differentiated it from erosion. This form of corrosion accounts for carbon steel pipe thickness reduction and can lead to ductile failure. It has been reported that carbon steel flow lines used as means of transporting hydrocarbon are susceptible to internal corrosion [14]. When considering coated flow lines, mass transfer of corrosive materials such as CO_2 has been identified as a means of reducing the integrity of pipelines because of the peeling off of protective inhibitor films and erosion of already formed layers of corrosion products [15,16]. Zhu et al. [17] emphasized the relationship that exists between corrosion in flow lines and mass transport. They also identified migration, diffusion and convection as processes responsible for mass transportation of ions in aqueous media. Sk et al. [18] stated the gaps present in most models that attempt to compute the corrosion rate from first principles and the resulting effect in using these models. The role of temperature was continuously mentioned in their study as a contributing factor. Saxena et al. [19] justified their assertion by concluding that the rate of corrosion in carbon steel increases 5.3 and 3.7 times as the temperature and flow increase, respectively.

Hasan et al. [20] explained piping process from wellhead to distribution flow lines. They addressed the limitations encountered in establishing a relationship between integrity and design of these pipelines and flow lines. The common practice has been to include an allowance/thickness in design that will serve as a preventive measure against corrosion because these lines are subject to deterioration by reason of their applications. Also, the possible uncertainties that result from not considering the localized effect of corrosion were outlined and grouped into four. Olajire [21] emphasized the environmental, technical and economic importance of corrosion control in metallic structures. Developing a single model to predict corrosion cases encountered in metal steel is difficult because of the random nature of corrosion and the difficult field conditions making the prevention of corrosion almost impossible [22]. According to Papavinasam [23], internal corrosion accounts for 57.7% of production pipeline failure in Alberta, Canada. It was also noted that total annual cost of corrosion in United States Transmission Pipeline sector is estimated to be in the range of 5391 to 6973 Million dollars. The percentage failure due to internal corrosion for Alberta, Canada from 1980 to 2005 is shown in the Fig. 1.

From literature, it can be inferred that the best form of corrosion control involves assessment/inspection of the metal, detection or ascertaining the type of damage or corrosion, monitoring the developmental stages of the corrosion products and managing/taking appropriate steps to save the situation. The best means of achieving these task is to develop a model from real time data obtained from the field. Operators can only state with assurance that a particular model best suits the prediction of flow line and pipeline corrosion if they are developed in-situ.

The aim of the study is to develop a model that predicts the corrosion rate in flow lines as a function of the operating temperature and concentration of CO_2. The type of corrosion considered is internal corrosion on curvilinear pipes, hence the reason behind this study.

2. Theoretical principle/method

In order to achieve the objectives within the scope of this research, non-linear regression data was employed. Also, the principle of

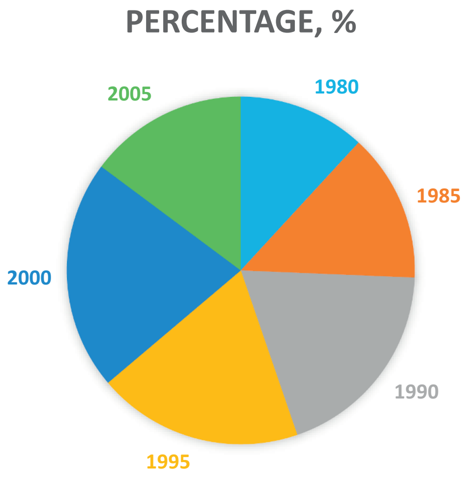

Fig. 1. Internal Corrosion failures over an interval of five years [23].

linear polarization resistance was used, in which the electrical conductivity (the reciprocal of resistance) of a fluid was related to its corrosiveness. A small potential that is within the range of 20 mV (which does not affect the natural corrosion process), was applied between the elements and the resulting current was measured. The polarization resistance is the ratio of the applied potential and the resulting current level. The measured resistance is inversely related to the corrosion rate. The electrical resistance of any conductor is given by:

$$\mathrm{R} = \frac{V}{I} \tag{1}$$

where:

R = Effective instantaneous resistance
V = Applied voltage
I = Instantaneous current between electrodes
The corrosion current (I_{CORR}), generated by the flow of electrons from anodic to cathodic sites, could be used to compute the corrosion rate by the application of a modified version of Faraday's Law

2.1. *Estimation of corrosion rate from corrosion current*

According to Faraday's Law:

$$\mathrm{Q} = {}^{nFW}\!\big/_{M} \tag{2}$$

where:

Q = Coulombs
n = Number of electrons involved in the electrochemical reaction
F = Faraday constant, 96,487 coulombs
W = weight of the electro active species
M = Molecular weight

From (2)

$$\mathrm{W} = {}^{QM}\!\big/_{nF} \tag{3}$$

Since the equivalent weight of electro active species to number of electrons (E.W) = M/n, then.

$$\mathrm{W} = {}^{Q \times E.\ W}\!\big/_{F} \tag{4}$$

Since Q = I*t from Faraday's Law, it implies:

$$\mathrm{W} = {}^{It \times E.\ W}\!\big/_{F} \tag{5}$$

From (5), the Corrosion Rate (C.R) can be expressed as W/t in grams/s. It is convenient and traditional to express corrosion rate in milli-inches per year (mpy). These units provide an indication of the degree of penetration of the corrosion damage over a year.

Dividing Eq. (5) by the electrode area and the density gives:
C.R in cm, then,

$$\mathrm{C.\ R.\ (cm/s)} = {}^{I * (E.\ W)}\!\big/_{dFA} \tag{6}$$

where:

d = density (g/cm^3)

Convert *sec*onds to years and centimeters to milli-inches. Convert the Faraday (amp-sec/eq) to micro amperes. Then,

$$\mathrm{C.\ R.\ (mpy)} = {}^{I(E.\ W) \times 31600000}\!\big/_{dFA \times 2500000} \tag{7}$$

Express the terms I/A as current density. Combining all the constants gives.

$$\text{Corrosion Rate (mpy)} = 0.13\ I_{CORR}\ (\mathrm{E.\ W})/\mathrm{d} \tag{8}$$

where:

$\mathbf{I_{CORR}}$ = corrosion current density, μA/cm^2
E.W = equivalent weight of corroding species, g

d = density of corroding species, g/cm^3
Eq. (8) was used to calculate the corrosion rate directly from I_{CORR}

2.2. Electrochemical corrosion theory

According to the mixed potential theory, any electrochemical reaction can be divided into two or more oxidation and reduction reactions and there can be no accumulation of electrical charge during the reaction (note that, this electrochemical reaction takes place in the absence of any externally applied potential). Thus, in a corroding system, oxidation of the metal (corrosion) and reduction of some species in solution are taking place at the same rate and the net measurable current is zero.

$$I_{MEAS} = I_{RED} - I_{OX} = 0 \tag{9}$$

Electrochemically, corrosion rate measurement is based on the determination of the oxidation current by the corrosion potential. The oxidation current is now identified as the corrosion current, I_{CORR}. Eq. (9) may now be rewritten as:

$$I_{MEAS} = I_{CORR} - I_{RED} = 0 \tag{10}$$

2.3. Model formulation

In order to find a functional relationship between corrosion rate in flow lines and other variables such as the flow line operating temperature and the partial pressure of CO_2, the nonlinear regression analysis was used as given by (11).

$$CR = a_o + a_1(T/p_{CO_2}) + a_2(p_{CO_2}/T) + a_3/(T \cdot p_{CO_2}) \tag{11}$$

The least-square minimization to solve Eq. (11) can be formulated as follows. An objective function $F(c)$ is first defined:

$$F(c) = r^T r \tag{12}$$

where, the vector $c = [a_0, a_1, a_2, a_3]$ represents 4 independent variables called regression constants. The elements of ***r*** are dependent variables called residues. The residue expresses the relative difference between the corrosion rate history (T, p_{CO_2}, CR) and the corresponding simulated corrosion rate $\widehat{CR}(T, p_{CO_2}, c)$. The residue for M number of data points is defined by

$$r_i = \frac{w_i\,[\widehat{CR}(T, p_{CO_2}, c)_i - CR(T, p_{CO_2})_i]}{CR(T, p_{CO_2})_i}, \quad i = 1, 2, 3, \cdots, M \tag{13}$$

where, w_i is a weight value.

Usually the simulated corrosion rate and the objective function are non-linear functions of the regression parameters, and as such, an iterative process is required. The nonlinear optimization requirement then is to find the update;

$$c_{i+1} = \arg\min\{F(c)\} \tag{14}$$

To prevent convergence to an unrealistic minimizer, the nonlinear optimization is controlled to enforce the descent direction such that the objective function at an iteration stage is greater than the objective function at the next iteration stage, that is, $F(c_{k+1}) < F(c_k)$. Once, the descent direction is located, a step size that would give a good decrease in the objective function is chosen.

If it is assumed that $F(c^k)$ is continuous, and that its first and second derivatives exist, a minimum of $F(c^k)$ can only be found at a stationary point. That is a point where

$$\frac{\partial F(c^k)}{\partial c_j} = 0 \quad j = 1, 2, \cdots, N \tag{15}$$

I spans from 1 to 3 while j runs from 1 to 2, why? Shouldn't j go from 1 to 3 as well?

$F(c^k)$ is expanded using Taylor series around the kth iteration c^k, by truncating at the second term whilst ignoring third and higher order terms.

$$F(c + \Delta c)^k = F(c^k) + \Delta c^k \cdot \nabla F(c^k) + 0.5(\Delta c^k)^2 \cdot \nabla^2 F(c^k) + (O)^3 \tag{16}$$

The first and second derivatives of $F(c^k)$ are described as follows:

$$\nabla F(c^k) = 2J(c^k)^T r(c^k) \tag{17}$$

$$\nabla^2 F(c^k) = 2[J(c^k)^T J(c^k) + Q(c^k)] \tag{18}$$

where the elements of the Jacobian Matrix ***J*** are

$$J(c^k)_{ij} = \frac{\partial r(c^k)_i}{\partial c_j} \tag{19}$$

Eq. (19) is the Hessian matrix ***H*** of second derivatives of ***F*** with respect to the parameter c^k. Matrix ***Q*** is defined from (20).

Table 1
The field gas conditions, composition, and properties.

Sample source		Gas treatment plant
Sampling temperature		25 °C
Sampling pressure		65 bar
Date collected		30th March., 2018
S/N	Composition	Mole %
1	Methane	**88.94**
2	Ethane	6.35
3	Propane	0.81
4	N-butane	0.23
5	ISO-butane	0.16
6	N-pentane	0.07
7	ISO-pentane	0.09
8	C6 +	0.03
9	CO2	2.56
10	Oxygen	0.00
11	Nitrogen	0.76
	Total	1000
Thermochemsitry		
1	Average Molecular Weight (g/mol)	18.24
2	Specific Gravity	0.631
3	Moisture Content (Ib/MMSCF)	2.90
4	Higher Heating Value (BTU/SCF)	1055.93
5	Wobbe Index (Higher Heating Value Basis)	1329.92

$$Q(c^k) = \sum_{i=1}^{M} r_i(c^k)\cdot\nabla^2 r_i(c^k) \tag{20}$$

The elements of $\boldsymbol{Q}$ are difficult to obtain, and since they are assumed to be small, $\boldsymbol{Q}$ is neglected. At first sight, this seems to be a good approximation only close to the solution. However, since the residuals usually are rather evenly distributed between positive and negative values, it is in general a fair approximation unless the data set includes systematic errors. The real data from a flow station used for development and validation of the developed model is tabulated in Table 2.

2.4. Field corrosion data

The gas composition showing the different compounds and the mole percent for the field is tabulated in Table 1. These compositions are used to calculate the partial pressure of each component present in the gas mixture.

According to Department of Petroleum Resources (DPR) Nigeria, every Exploration and Exploitation facility is expected to conduct field test on their facilities every 3–5 years. Though, most of the materials used in these facilities are expected to resist corrosion for 20–25 years. The baseline data for comparison are gotten from the standard schedule (thickness) and standard schedule tables. The flow line under consideration in this study is about 3 km with 2-in. diameter (Fig. 2).

The standard for calculating the rate of corrosion for pipeline and process piping is detailed in API 570. Long range ultrasonic testing (LRUT) screening tool for pipework was initially applied in the location of study (Fig. 3). It can examine large volumes of material from a single location, but the product used in this study can only travel 50 m interval at a run. It works with the principle of sound wave propagation. These waves can travel 50 m with minimal attenuation and it offers the potential of testing large areas from a single point using a pulse-echo transducer bracelet wrapped around the pipe.

The original thickness of the flow line is used to calibrate the tool before scanning; and while scanning, any section of the flow line with thickness less than the original thickness (Fig. 4) will be indicated on the monitor.

Having the constants fixed in Eq. (11), the model equation for the corrosion rate becomes:

$$\mathrm{CR} = -14.4251 + 0.8680\ \mathrm{T} + 82.8273\ \mathrm{P(CO_2)} \tag{21}$$

Note: In order to ensure unit consistency, a_1 has units of mass/temp.*cubic time, while a_2 has units of temp.*cubic time/mass and, a_3 has units of mass*temp./cubic time.

3. Results and discussion

The statistical analysis of data was done using Microsoft Excel statistical plug-in features while non-linear multiple regression

Table 2
Field data for this study.

S/N	Op. Temp [°C]	CO_2 Pressure [bar]	Corrosion Rate [mm/yr]	S/N	Op. Temp [°C]	CO_2 Pressure [bar]	Corrosion Rate [mm/yr]
1	30	4	3.2	14	34	6	5.3
2	30	4	3.1	15	34	6	5.2
4	30	4	3.1	17	36	7	6
5	30	4	3.2	18	36	7	6
6	32	5	4.1	19	36	7	6.1
7	32	5	4.1	20	36	7	6
8	32	5	4	21	36	7	6.1
9	32	5	4	22	37	8	7.6
10	32	5	4.1	23	37	8	7.5
11	34	6	5.2	24	37	8	7.6
12	34	6	5.2	25	37	8	7.5
13	34	6	5.1	26	37	8	7.5

Regression Const		Statistical Analysis	
a_0	−14.4251	No. of data points	26
a_1	0.867973	mean value	5.196154
a_2	82.82732	SSE	0.178562
a_3	1.653277	SST	58.51199
		R sq.	0.996948
		Variance	0.006868

Table 3
Validation of Model Estimates of Corrosion Rate with Field Measurements.

S/N	Corrosion rate [mm/yr]	Simulated corrosion rate	S/N	Corrosion rate [mm/yr]	Simulated corrosion rate
1	3.2	3.1421136	14	5.3	5.1181009
2	3.1	3.1421136	15	5.2	5.1181009
3	3.1	3.1421136	16	5.2	5.1181009
4	3.1	3.1421136	17	6	6.1506313
5	3.2	3.1421136	18	6	6.1506313
6	4.1	4.0820256	19	6.1	6.1506313
7	4.1	4.0820256	20	6	6.1506313
8	4	4.0820256	21	6.1	6.1506313
9	4	4.0820256	22	7.6	7.5034679
10	4.1	4.0820256	23	7.5	7.5034679
11	5.2	5.1181009	24	7.6	7.5034679
12	5.2	5.1181009	25	7.5	7.5034679
13	5.1	5.1181009	26	7.5	7.5034679

Table 4
Comparing Model Estimates with Field Data at Different Temperatures and CO_2 Partial Pressures.

S/N	Op. Temp [°C]	CO_2 pressure [bar]	Corrosion rate [mm/yr]	Simulated corrosion rate	S/N	Op. Temp [°C]	CO_2 pressure [bar]	Corrosion rate [mm/yr]	Simulated corrosion rate
1	30	4	3.2	3.1421136	14	34	6	5.3	5.1181009
2	30	4	3.1	3.1421136	15	34	6	5.2	5.1181009
3	30	4	3.1	3.1421136	16	34	6	5.2	5.1181009
4	30	4	3.1	3.1421136	17	36	7	6	6.1506313
5	30	4	3.2	3.1421136	18	36	7	6	6.1506313
6	32	5	4.1	4.0820256	19	36	7	6.1	6.1506313
7	32	5	4.1	4.0820256	20	36	7	6	6.1506313
8	32	5	4	4.0820256	21	36	7	6.1	6.1506313
9	32	5	4	4.0820256	22	37	8	7.6	7.5034679
10	32	5	4.1	4.0820256	23	37	8	7.5	7.5034679
11	34	6	5.2	5.1181009	24	37	8	7.6	7.5034679
12	34	6	5.2	5.1181009	25	37	8	7.5	7.5034679
13	34	6	5.1	5.1181009	26	37	8	7.5	7.5034679

Fig. 2. Section Picture of the Curvilinear Pipe.

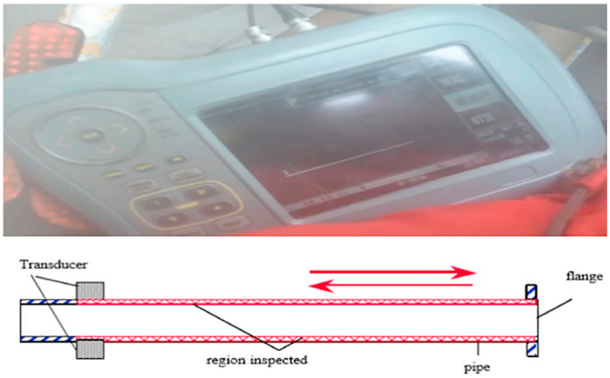

Fig. 3. 50 Meters range Ultrasonic testing of Flow Line.

Fig. 4. Section of the Flow Line with Large Internal Corrosion.

analysis was performed with the regression equation of the field data to ascertain possible relationships between the input and output variables. The validation of the estimated corrosion rates using the developed model as against field measurements is as given in Table 3, while Table 4 is the validation of model with field data at different temperatures and pressures.

Table 4 shows the operating temperature, partial pressure of CO_2 and corrosion data collected from a flow line facility. The corrosion data was used for the development of corrosion prediction model equation obtained in this work. A plot of temperature against corrosion rate as shown in Fig. 5 shows that the operating temperature of the fluid in the flow line has effect on corrosion rate of the pipe. Similarly, the plot of partial pressure of CO_2 in the fluid against corrosion rate shows that corrosion rate is also affected by the partial pressure of CO_2 in the flow line. The observed trends are in line with the findings of published literature [20,22] which established the effect of operating temperature and pressure on the rate of corrosion in a flow line. Fig. 6 illustrates the relationship between the actual and estimated corrosion rates against temperature. It shows that within the operating temperature range, the actual and estimated corrosion rates increased. Corrosion rate increased as temperature increased and it is such that for every 6 to 7 degrees' Celsius increase in temperature, the rate of corrosion is almost doubled and this is justified by the results in Table 4. This can be supported by the Arrhenius and Kinetic theories, because higher temperatures molecules gain greater amounts of energy hence,

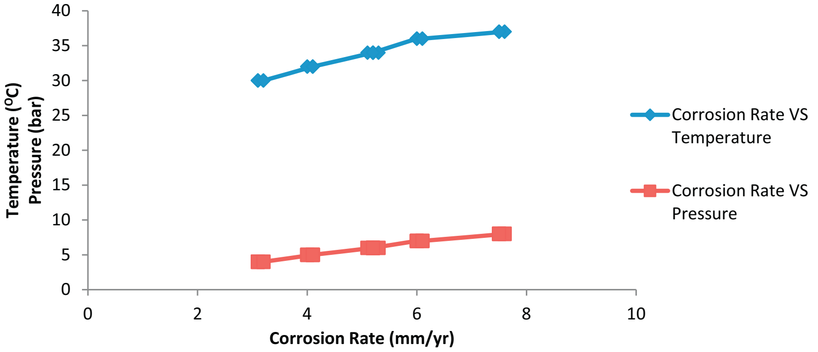

Fig. 5. Temperature and Partial Pressure of CO_2 vs Corrosion Rate.

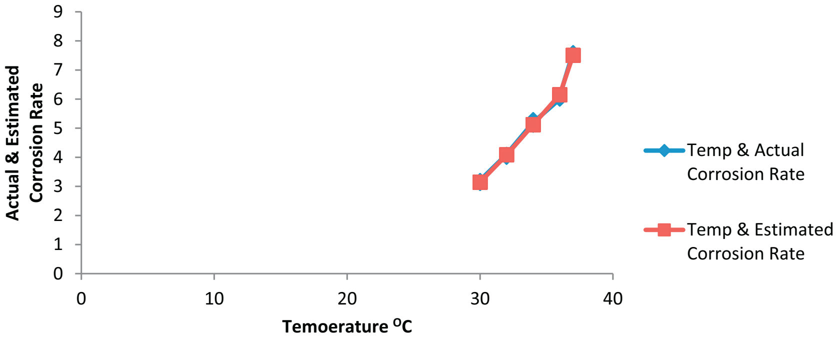

Fig. 6. Experimental and Model Estimates of Corrosion Rate vs Temperature.

the activation energy for electrochemical reaction is lowered thereby enabling fast collisions/reaction rates resulting in the appearance of corrosion deposits/products within shorter times. Temperature played an important role in the rate of corrosion. An increase in temperature boosts the reaction potential of iron in steel when the enabling conditions that favour corrosion become established; CO_2 can form carbonic acid when in contact with water in petroleum fluids tapped from gas condensate walls, and by nature, acids are corrosive which explains why the gas poses threat to petroleum pipes. Fig. 7 shows that actual and estimated corrosion rates increased with increase in the partial pressure of CO_2. Natural gas reservoirs usually contain undesirable quantities of CO_2 and the partial pressure of CO2 has been identified as one of the factors responsible for corrosion in flow lines. The CO_2 partial pressure influenced corrosion rate and since pressure increases with depth, points farther from the pipe exit experiences higher corrosion rates. Corrosion increased with partial pressure increment from 4 to 8 bar; and this lowers the corrosion resistance of the material of construction (iron in steel) of the flow line leading to pitting damage [23,24]. Therefore, the higher the CO_2 partial pressure, the more severe is the corrosion risk on the flow lines, as this directly translates to higher concentrations of carbonic acid which is a corrosion stimulant.

Fig. 6 shows a near linear relationship between the corrosion rate and the temperature of the flowing stream. This is in line with the observed trends of the De Waard model simulations and the results on the corrosion rate monograph. Similarly, Fig. 7 which is a plot of the flow line pressure against the actual and simulated corrosion rates, also shows a near linear relationship between the corrosion rate and the partial pressure of CO_2.

Temperature and pressure can influence the rate of corrosion directly, by speeding the process of corrosion; and indirectly, by

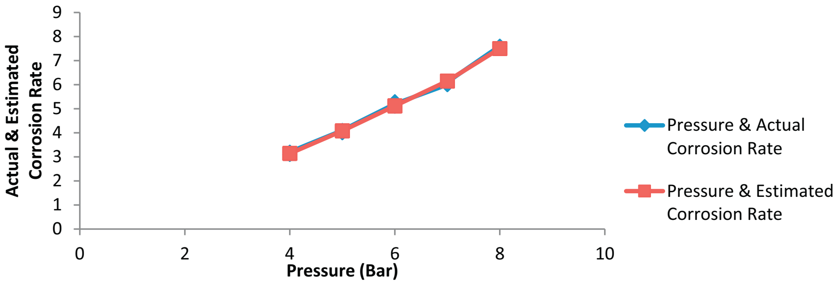

Fig. 7. Experimental and Model Estimates of Corrosion rate vs Pressure of CO_2.

affecting the scale formation. This leads to a higher rate of corrosion because the electrochemical reactions generally occur faster at higher temperature. Javidi and Bekhrad [25] identified C)2 corrosion as one of the main causes of failures for pipelines transportation and flow lines carrying gas.

3.1. Model validation with other field data

The corrosion rate model proposed in this study was validated with a field data from a pipeline integrity company located in Port Harcourt Rivers State, Nigeria.

S/N	Corrosion Rate, mm/yr	The Proposed Model
1	0.82	0.8109
2	0.40	0.3972
3	0.41	0.4101
4	1.16	1.1519
5	3.06	3.0512
6	1.95	1.9459
7	0.94	0.9311
8	1.78	1.7753

4. Conclusion

The ability to accurately predict and manage the corrosion rate of flow lines in a given environment is of great importance to the oil and gas industry. The basic approach used in this research work is the principle of nonlinear regression data analysis (NRDA). A corrosion rate model was developed which is given as; $CR = -14.4251 + 0.8680\,T + 82.8273\,P(CO_2)$.The simulated corrosion rate model was developed as a function of operating temperature and partial pressure of carbon (iv) oxide (CO_2). The actual corrosion rate was approximately the same as the simulated corrosion rate and the estimated variance is 0.006868, which is very low indicating that the model is accurate. The benefit of this model is that it helps in optimizing resources and gives room for proper planning in terms of taking proactive measures against pipeline corrosion/deterioration in the petroleum industry which will inturn conserve pipeline integrity. In addition, it is suggested that this model is tried on other production facilities that make use of flow lines with CO_2 as corrosive medium, in order to ascertain its extensive ability, flexibility and reliability as a tool of great importance for pipeline management.

Acknowledgment

The authors would like to thank Covenant University Centre for Research Innovation and Discovery (CUCRID) Ota, Nigeria for its support in making the publication of this research possible.

Appendix A. Supplementary data

Supplementary data to this article can be found online at https://doi.org/10.1016/j.engfailanal.2019.04.037.

References

[1] P. Li, Y. Zhao, B. Liu, G. Zeng, T. Zhang, D. Xu, H. Gu, T. Gu, F. Wang, Experimental testing and numerical simulation to analyze the corrosion failures of single well pipelines in Tahe oilfield, Eng. Fail. Anal. 80 (2017) 112–122.

[2] C.I. Ossai, B. Boswell, I.J. Dacies, Pipeline failure in corrosive environments-a conceptual analysis of trends and effects, Eng. Fail. Anal. 53 (2015) 36–58.

[3] N. Birbilis, M.K. Cavanaugh, A.D. Sudholz, S.M. Zhu, M.A. Easton, M.A. Gibson, A combined neural network and mechanistic approach for the prediction of corrosion rate and yield strength of magnesium-rare earth alloys, Corros. Sci. 53 (2011) 168–176.

[4] J. Wang, Y. Jang, G. Wan, V. Giridharan, G.L. Song, Z. Xu, Y. Koo, P. Qi, J. Sankar, N. Huang, Y. Yun, Flow-induced corrosion of absorbable magnesium alloy: in-situ and real-time electrochemical study, Corros. Sci. 104 (2016) 277–289.

[5] P. Hopkins, A. Cosham, How to assess defects in your pipelines using fitness-for-purpose methods, Conference on Advances in Pipeline Technology, IBC, Dubai, 1997September.

[6] P. Hopkins, Pipeline Integrity Reviews, Pipeline Pigging, Integrity Assessment and Repair Conference, February 2001, Houston, (2001).

[7] D. Drazic, Iron and its electrochemistry in an active state, Mod. Asp. Electrochem 19 (1989) 62–192.

[8] Y. Zheng, B. Brown, S. Nesic, Electrochemical study and modeling of H2S corrosion of mild steel, Corrosion 70 (2014) 351–365.

[9] National Association of Corrosion Engineers, Annual Corrosion Conference and Exposition: Water and Wastewater industries, NACE-96027, Denver, United States, 24-29 Mar 1996.

[10] A. Kahyarian, M. Achour, S. Nesic, CO2 corrosion of mild steel, in: A.M. El-Sherik (Ed.), Trends Oil Gas Corros. Res. Technol, Elsevier, 2017, pp. 149–190.

[11] A. Kahyarian, M. Achour, S. Nesic, Mathematical modeling of uniform CO2 corrosion, in: A.M. El-Sherik (Ed.), Trends Oil Gas Corros. Res. Technol, Elsevier, 2017, pp. 805–849.

[12] American Petroleum Institute, PPTS operator advisory: the ins and outs of corrosion releases, PPTS Advisory 2014–1, April, (2014).

[13] V. Kain, Flow accelerated corrosion: Forms, mechanisms and case studies, 1st International Conference on Structural Integrity, ICONS, Procedia Engineering, vol. 86, 2014, pp. 576–588.

[14] W. Li, B.F.M. Pots, B. Brown, K.E. Kee, S. Nesic, A direct measurement of wall shear stress in multiphase flow-Is it an important parameter in CO2 corrosion of carbon steel pipelines? Corros. Sci. 110 (2016) 35–45.

[15] V. Ruzic, M. Veidt, S. Nesic, Protective iron carbonate films – part 1: mechanical removal in single-phase aqueous flow, Corrosion 62 (2006) 419–432.
[16] E. Gulbrandsen, A. Gtana, Testing of carbon dioxide corrosion inhibitor performance at high flow velocities in jet impingement geometry. Effects of mass transfer and flow forces, Corrosion 63 (2007) 1009–1020.
[17] Y. Zhu, M.L. Free, R. Woollam, W. Durnie, A review of surfactants as corrosion inhibitors and associated modeling, Prog. Mater. Sci. 90 (2017) 159–223.
[18] M.H. Sk, A.M. Abdullah, M. Ko, B. Ingham, N. Laycock, R. Arul, D.E. Williams, Local supersaturation and the growth of protective scales during CO_2 corrosion of steel: effect of pH and solution flow, Corros. Sci. 126 (2017) 26–36.
[19] R.C. Saxena, J. Biswal, H.J. Pant, J.S. Samantray, S.C. Sharma, A.K. Gupta, S.S. Ray, Application of thin layer activation technique for monitoring corrosion of carbon steel in hydrocarbon processing environment, Appl. Radiat. Isot. 135 (2018) 201–206.
[20] S. Hasan, L. Sweet, J. Hults, G. Valbuena, B. Singh, Corrosion risk-based subsea pipeline design, Int. J. Press. Vessel. Pip. 159 (2018) 1–14.
[21] A. Olajire, Corrosion inhibition of offshore oil and gas production facilities using organic compound inhibitors – a review, J. Mol. Liq. 248 (2017) 775–808.
[22] H.R. Vanaei, A. Eslami, A. Egbewande, A review on pipeline corrosion, in-line inspection (ILI), and corrosion growth rate models, Int. J. Press. Vessel. Pip. 149 (2017) 43–54.
[23] Sankara Papavinasam, Corrosion Control in the Oil and Gas Industry, Gulf Professional Publishing, 2014.
[24] H. Bai, Y. Wang, Y. Ma, Q. Zhang, N. Zhang, Effect of CO2 partial pressure on the corrosion behavior of J55 carbon steel in 30% crude oil/brine mixture, Materials 11 (2018) 1765, https://doi.org/10.3390/ma11091765.
[25] M. Javidi, S. Bekhrad, Failure analysis of a wet gas pipeline due to localized CO2 corrosion, Eng. Fail. Anal. 89 (2018) 46–56.